Non-orthogonal Corneal Astigmatism among Normal and Keratoconic Brazilian and Chinese Populations

Ahmed Abass[1*], John Clamp[2], FangJun Bao[3], Renato Ambrósio Jr[4], Ahmed Elsheikh[1,5]

[1] School of Engineering, University of Liverpool, Liverpool, L69 3GH, UK
[2] UltraVision CLPL, Leighton Buzzard, LU7 4RW, UK
[3] Eye Hospital, WenZhou Medical University, WenZhou, China
[4] Federal University of São Paulo, São Paulo, Brazil
[5] National Institute for Health Research (NIHR) Biomedical Research Centre at Moorfields Eye Hospital NHS foundation Trust and UCL Institute of Ophthalmology, London, EC1V 2PD, UK

[*] **Author for correspondence:**
Ahmed Abass
School of Engineering, University of Liverpool, Liverpool, L69 3GH, UK.
A.Abass@liverpool.ac.uk

Keywords: cornea; astigmatism; non-orthogonal astigmatism; optical power

Number of words: 4586

Abstract

Purpose: To investigate the prevalence of non-orthogonal astigmatism among normal and keratoconic Brazilian and Chinese populations

Methods: Topography data was obtained using the Pentacam High Resolution (HR) system ® from 458 Brazilian (aged 35.6±15.8 years) and 505 Chinese eyes (aged 31.6±10.8 years) with no history of keratoconus or refractive surgery, and 314 Brazilian (aged 24.2±5.7 years) and 74 Chinese (aged 22.0±5.5 years) keratoconic eyes. Orthogonal values of optical flat and steep powers were determined by finding the angular positions of two perpendicular meridians that gave the maximum difference in power. Additionally, the angular positions of the meridians with the minimum and maximum optical powers were located while being unrestricted by the usual orthogonality assumption. Eyes were determined to have non-orthogonal astigmatism if the angle between the two meridians with maximum and minimum optical power deviated by more than 5° from 90°.

Results: Evidence of non-orthogonal astigmatism was found in 39% of the Brazilian keratoconic eyes, 26% of the Chinese keratoconic eyes, 29% of the Brazilian normal eyes and 20% of the Chinese normal eyes.

Conclusions: The large percentage of participants with non-orthogonal astigmatism in both normal and keratoconic eyes illustrates the need for the common orthogonality assumption to be reviewed when correcting for astigmatism. The prevalence of non-orthogonality should be considered by expanding the prescription system to consider the two power meridians, and their independent positions.

Introduction

Astigmatism was first reported by Thomas Young in 1801 (1, 2), and corrected by cylindrical lenses by George Airy in 1872 (3). Astigmatism is an optical refractive error, which develops when the shape of the eye's refractive components, primarily the cornea and crystalline lens, deviate from being rotationally symmetric. There is wide prevalence of astigmatism worldwide and estimates commonly exceed 30% of the population depending on the astigmatism power threshold adopted in each study (0.5 or 1.0 dioptre) (4-8).

"Astigmatism axis" is the term used to describe the angular position of cornea's meridian with the highest optical power. Its angle is measured in a counter-clockwise direction from a horizontal line at the level of the pupil centre as seen by an observer with direction 0° being on the right of the eye. Regular orthogonal astigmatism – where the angle between the meridians with the highest and lowest optical powers (flattest and steepest meridians, respectively) is 90° – is commonly assumed in normal eyes. Therefore, the current eye refractive prescription system is based on correcting astigmatism using orthogonal double power lenses known as toric or sphero-cylindrical lenses (9).

Zernike polynomials and Fourier series are commonly used to provide a quantitative evaluation of corneal irregularity (10). However, while they have clear benefits in corneal topography analysis, they mask non-orthogonal astigmatism due to their reliance on orthogonal functions. Non-orthogonal astigmatism cannot be quantified distinctly by Zernike polynomials as it is usually included among high order aberration terms. However, irregular astigmatism can be quantified in polar coordinates at each corneal mire ring 'i' by fitting corneal power map to the Fourier equation:

$$F_i(\alpha) = C_0 + C_1 \cos(\alpha - \beta_1) + C_2 \cos 2(\alpha - \beta_2) + C_3 \cos 3(\alpha - \beta_3) \qquad \textit{Equation 1}$$

in which C_3 represents irregular astigmatic component and α is the angular position. In this equation, coefficients C_0, C_1 and C_2 provide the spherical, the decentration and the regular orthogonal astigmatic components at the mire ring 'i', while phase angles β_1, β_2, and β_3

represent the decentration, the axis of regular orthogonal astigmatism and hypothetical axis of irregular astigmatism, respectively.

Some corneal topographers provide an irregularity index which is the Fourier's function coefficient C_3 divided by the average corneal dioptric power. The index is dependent on the device's hardware and the signal processing algorithm embedded in its software (11). For example, factors including the topographer resolution or the number of the mire rings and their positions could significantly affect the irregularity index and make it less useful when extrapolated to another videokeratographer (12). Further, there is no clinical information that can be directly taken from the irregularity index except by correlating it statistically to other measurable clinical data (13). Mathematically, Fourier series coefficient β_3 is intended to provide information on the polar distribution of irregular astigmatism but not about the irregular astigmatism phase or the non-orthogonal astigmatism. In fact, the existing literature which evaluates corneal irregularity by Fourier series harmonic ignores the irregular astigmatism phase angle β_3 and does not associate it with a specific physical meaning (11, 14, 15). While it is acknowledged that a quantitative degree of irregularity in refractive power exists in normal eyes and this knowledge have been simulated by mathematical modelling (16), no technique is available to locate the axes of irregular astigmatism. As a result, irregular astigmatism cannot be fully corrected by existing spectacle lenses and a degree of astigmatism will remain after correction.

This study aims to explore the validity of the common orthogonality assumption in large populations of both normal and keratoconic eyes. Considering the variable sensitivity of different methods that map corneal refractive power (17, 18), the power maps generated in this study used axial curvature. For each cornea included in the study, analysis of the power map led to estimated orientations of the flattest and steepest meridians while adopting and ignoring the orthogonality assumption. The results not only estimated the percentage of eyes, for which the orthogonality assumption is not valid, but also quantified the effect of the assumption on the magnitude and direction of astigmatism.

Materials and Methods

Participants

This study was conducted according to the tenets of the Declaration of Helsinki. However, the institutional review board ruled that approval was not required for this record review study, each participant provided a signed consent form for the use of his data for research purposes before his details were anonymised. Due to the reported topographical and anatomical differences between Caucasian and Chinese populations (19-21), both Caucasian (from Brazil) and Chinese populations were considered in this study to investigate if results were attached to a certain population. The study included 772 Brazilians and 579 Chinese with or without keratoconus, Table 1. The participants were selected from referrals to Hospital de Olhos Santa Luzia, Maceio, Alagoas, Brazil, and the Eye Hospital, WenZhou Medical University, Wenzhou, China. The exclusion criteria included current ocular diseases, history of trauma or ocular surgery, intraocular pressure (IOP) above 21 mmHg as measured by Ocular Response Analyser (Reichert Technologies, Depew, USA), soft contact lens wear until less than 2 weeks before topography measurement and rigid, gas-permeable (RGP) contact lens wear until less than 4 weeks before topography measurement. An inclusion criterion for keratoconic participants was a clear presence of keratoconus with no previous ocular procedures, such as collagen cross-linking. One randomly selected eye of each participant was included in the study and scanned using the Pentacam HR Scheimpflug tomographer (OCULUS Optikgeräte GmbH, Wetzlar, Germany). Where a participant had a single keratoconic eye, this eye was selected. At least, three successive scans were taken for each participant with approximately time period of half a minute among them. The measurements continued until three scans with an instrument-generated quality factor of at least 95% and 90% were obtained for the anterior and posterior surfaces, respectively. Scans that had an examination quality status identified as “OK” by the Pentacam Software were considered and analysed individually, however, the average of the outcomes of three successful scans for

each eye were considered in the result. Room lights were switched off during data acquisition. Participants were asked to sit in front of the instrument while its level was being adjusted to suit the participant's eye. Participants were asked to put their chin on the chin rest and their forehead on the forehead rest. Fine alignment was carried out by the Pentacam joystick while participants were asked to fixate on a target at the centre of the instrument camera. Subjects were asked to blink and reposition themselves between each shot while the instrument was pulled back fully then realigned. The clinical characteristics of the subjects as measured by the Pentacam HR system are presented in Table 2 where the topographical keratoconus classification (TKC) range was identified between level 1 and level 3 to 4 (3.5) among both Brazilian and Chinese participants. The frequency distribution of the level for keratoconic patents is presented in Figure 1. Non-extrapolated elevation data for both the anterior and posterior surfaces were exported in comma-separated values (CSV) format and analysed using a custom-built Matlab 2017 code (MathWorks, Natick, USA).

Power maps

Corneal axial curvatures were calculated for 360 meridians, with a one degree angular step, covering the measured area of the cornea. Centres of axial curvatures were assumed to lie on the corneal optical axis (22). As illustrated in Figure 2, the axial radius of curvature at any point is calculated as:

$$R = \frac{x}{\cos\left(\frac{\pi}{2} - \alpha\right)} \qquad \textit{Equation 2}$$

Where x is the distance from the corneal centre to the point of calculation and α is the tangent angle at this point. This process was carried out for both corneal anterior and posterior surfaces and the corresponding radii of curvature, $R_{anterior}$ and $R_{posterior}$, were used to calculate the corneal optical power P using the Gaussian optics formula (23, 24):

$$P = \frac{n_{cornea} - n_{air}}{R_{anterior}} + \frac{n_{aqueous} - n_{cornea}}{R_{posterior}} - \frac{t_c}{n_{cornea}} \times \frac{n_{cornea} - n_{air}}{R_{anterior}} \times \frac{n_{aqueous} - n_{cornea}}{R_{posterior}} \quad \textit{Equation 3}$$

where the refractive indices of air, n_{air}, cornea, n_{cornea}, and aqueous, $n_{aqueous}$, were set at 1.0, 1.376 and 1.336, respectively, following Gullstrand's relaxed eye model (25, 26), Figure 3. The central corneal thickness, t_c, was measured by the Pentacam HR Scheimpflug system.

Analysis of power maps

The meridians with the flattest and steepest powers were located within the central pupil area of the cornea with a 3mm diameter (27) by first averaging the power along 180 meridians with an angular step of one degree. This leads to meridians M = [M_0, M_1, ……, M_{179}] that correspond to angles Θ = [0°, 1°, ……, 179°] and have average refractive powers PM = [P_0, P_1, ……, P_{179}], respectively. The commonly-used orthogonal optical power orientation can be calculated by first splitting the meridional averaged refractive powers into two perpendicular groups PM_a (= [P_0, P_1, ……, P_{89}]) and PM_b (= [P_{90}, P_{91}, ……, P_{179}]). The absolute optical power difference between the two groups can then be determined as:

$$\Delta PM = |PM_a - PM_b| \quad \textit{Equation 4}$$

When the maximum value of ΔPM is reached, the corresponding two orthogonal meridians, from the two groups PM_a and PM_b, are considered to represent the flattest and steepest (or steepest and flattest) orthogonal meridians in the cornea, Figure 4a.

On the other hand, the non-orthogonal flattest and steepest power meridians are free from the condition of orthogonality and are located by simply finding the maximum and minimum values of PM (Figure 4b). In this case, the absolute optical power difference, ΔP, the absolute angle separating the flattest and steepest meridians, $\Delta\theta$, and the absolute acute angle, φ, between the two meridians are determined with Equation 5, Equation 6 and Equation 7, respectively.

$$\Delta P = \left|P_{flat} - P_{steep}\right| \quad \textit{Equation 5}$$

$$\Delta\theta = \left|\theta_{flat} - \theta_{steep}\right| \qquad \textit{Equation 6}$$

$$\varphi = \begin{cases} \Delta\theta, & \Delta\theta \leq 90^{\circ} \\ 180^{\circ} - \Delta\theta, & \Delta\theta > 90^{\circ} \end{cases} \qquad \textit{Equation 7}$$

Statistical analysis

Statistical analysis was performed using Matlab Statistics and Machine Learning Toolbox (MathWorks, Natick, USA). The null hypothesis probability (p) at 95% at confidence level was calculated. Two sample t-test was used to investigate the significance between pairs of data sets to check whether the results represent independent records. The probability p is an element of the period [0,1] where values of p higher than 0.05 indicates the validity of the null hypothesis (28).

Results

The angular difference, φ, between the main power meridians showed significant reductions when considering non-orthogonal astigmatism compared with the common orthogonal assumption – and this was true for both normal and keratoconic corneas, and for both populations (p=0), Table 3. However, the variations in optical difference between considering non-orthogonal and orthogonal astigmatism were not significant and remained below the clinically correctable astigmatic power in all groups except normal Chinese corneas (p=0.015). Further, while the variations in power difference were small in normal corneas (Brazilian group: 0.07±0.1D, Chinese group: 0.08±0.08D), the effect was much smaller in keratoconic corneas (Brazilian group: 0.03±0.0D, Chinese group: 0.02±0.05D).

Since the minimum astigmatic power that can be corrected clinically is 0.5D (29) and a significant part of the human population have uncorrected astigmatism of up to 1.0D with no notable effect on their visual acuity (8, 30, 31), 1.0D was considered in this study as the threshold that separated clinically astigmatic and non-astigmatic eyes. Applying this threshold to the analysis results of normal and keratoconic corneas, based on orthogonal and non-

orthogonal power axes, showed that more Chinese corneas would be considered astigmatic when their power axes were calculated non-orthogonally (p=0.028), Figure 5. Removing the orthogonality condition increased the percentage of astigmatic corneas in normal Chinese participants by 6% (p=0.028). Meanwhile, there was no significant corresponding effect in normal Brazilian eyes (0.0507) and keratoconic eyes of both Brazilian (p=0.899) and Chinese (p=1) populations.

In order to evaluate the significance of this finding, the acute angle φ was plotted against the relevant absolute power difference ΔP for both Brazilian and Chinese populations in Figure 6 and Figure 7. In these figures, the corneas were divided into three groups, no or mild astigmatic corneas ($\Delta\mathrm{P} \leq 1\mathrm{D}$), regular astigmatic corneas (with $90° \geq \varphi \geq 85°, \Delta\mathrm{P} > 1\mathrm{D}$), and irregular astigmatic corneas (with $\varphi < 85°, \Delta\mathrm{P} > 1\mathrm{D}$). According to this classification, 29% of normal Brazilian, 39% of keratoconic Brazilian, 20% of normal Chinese and 26% of keratoconic Chinese participants had non-orthogonal astigmatism with an optical power difference >1D between the main power meridians and an acute angle $\varphi < 85^\circ$.

In addition, 29% of normal Brazilian, 39% of keratoconic Brazilian, 20% of normal Chinese and 26% of keratoconic Chinese participants had non-orthogonal astigmatism with an optical power difference bigger than 1D between the main power meridians and an acute angle $\varphi < 85^\circ$. On the other hand, regular astigmatism, with $\varphi \geq 85^\circ, \Delta\mathrm{P} > 1\mathrm{D}$, was identified as 17% of normal Brazilian, 50% of keratoconic Brazilian, 10% of normal Chinese and 72% in keratoconic Chinese.

Discussion

The assumption of orthogonality between steep and flat meridians in corneal power maps has been a common feature in the analysis of astigmatism and in clinical techniques to determine

the eye's visual acuity, although possible meridional non-orthogonality has been identified earlier (11, 14, 32-34). Optical power non-orthogonality was acknowledged in the literature as a contributing factor to high order aberrations and identified by indices that do not provide clinical parameters like refractive power or axis angle. Despite of being expressed quantitatively and statistically by a normalised Fourier series coefficient called the irregularity index, no expression of non-orthogonal astigmatism magnitude or axis angle has been presented. Moreover, the widespread use of Zernike and Fourier functions, which primarily consist of series of orthogonal sinusoidal terms, to characterise corneal irregularity leads to the consideration of non-orthogonal astigmatism as a high order aberration phenomenon that cannot be corrected by toric refractive lenses (11, 35). As a result, non-orthogonal astigmatism, where it exists, may be causing residual astigmatism, even among normal eyes. The plan in this study was to take a step back and identify the cornea's flattest and steepest refractive power meridians without forcing them to be orthogonal as a better representation of astigmatism.

Starting with the traditional orthogonal analysis, this study showed mean frequency percentages of astigmatism among normal Brazilian and Chinese participants of 44% and 24%, respectively. Among keratoconic participants, the mean percentages were up to 89% in Brazilian participants and 97% in Chinese participants. Considering non-orthogonal analysis, by removing the restriction of orthogonality of optical power meridians, the clinical data showed non-significant increases in mean frequency percentages of astigmatism among normal Brazilian and Chinese participants of 2% (up to 46%, p=0.97) and 6% (up to 30%, p=0.29), respectively. In contrast, no corresponding changes were found in the keratoconic participants of both populations. This last observation was possibly caused by the mean frequency percentages in keratoconic eyes being already high with the orthogonality assumption.

However, by using non-orthogonal analysis to determine the absolute acute angle φ between the flattest and steepest power meridians, the mean values of φ were below 90° by 16.4±13.1° among normal Brazilian participants (range = 0 - 59°), 19.4±13.5° in normal Chinese

participants (range = 0 - 58°), 7.5±8.2° in keratoconic Brazilian participants (range = 0 - 45°) and 4.6±4.8° in keratoconic Chinese participants (range = 0 - 23°). These results illustrate the non-orthogonality of the cornea's main power meridians, especially in non-keratoconic eyes. Looking at Figures 6, 7 and considering the shape of the eye, and the fact that regular astigmatism is more common than irregular astigmatism, it is expected that very steep meridians are more likely to be more perpendicular to flat meridians than the less steep ones regardless of the instrument used. Furthermore, when there is a relatively low cylinder, there is more variability on the axis. Even though the study showed that the percentage of non-orthogonal corneal astigmatism in keratoconic eyes was 6% to 10% higher than in normal eyes, the magnitude of the astigmatism among keratoconic populations (10.0D among Brazilian participants, 8.8D among Chinese participants) was more than double that in normal populations (3.8D among Brazilian participants, 2.3D in among Chinese participants). The small magnitude of astigmatism in normal eyes is a possible contributing factor for not identifying its non-orthogonality compared to keratoconic eyes where there is significantly larger astigmatism. It is also normal among all measurements that measuring large values is technically easier than measuring small values as the signal-to-noise-ratio of large values is higher. These results could have important implications on prescription systems to correct vision errors. The current system relies on three values; *Sphere*, *Cylinder* and *Axis*, which describe the spherical error (*Sphere*) and the two orthogonal powers: [P1= *Sphere* at angle *Axis* + 90°] and [P2 = *Sphere* + *Cylinder* at angle *Axis*]. The results of the present study illustrate the importance of considering the non-orthogonality of the main power meridians, possibly making it necessary to increase the prescription system figures to four; [P1@*Axis1*] and [P2@*Axis2*], where *Axis1* and *Axis2* represent the angles of the steepest and flattest meridians, respectively. This system would allow the angle between the power meridians to differ from 90^{o} (36) in line with the topography findings presented herein.

Using the axial curvature method to map corneal power in this study was based on its effectiveness in representing the overall visual acuity due to considering the optical axis as a reference in power calculations and assuming that centres of axial curvature always lay on this axis (18, 37). Other mapping methods were excluded for different reasons; simulated keratometry (sim-k) for fitting a unique curvature to each power meridian (38, 39), the tangential curvature for its sensitivity to the digital noise associated with videokeratographers' data and not being sensitive to optical axis position (22, 40), and the light ray tracing for its sensitivity to numerical errors near the centre of calculations at the optical axis where the corneal focal point is close to mathematical infinity (41). Because of their inherent assumptions, the simulated keratometry (sim-k) optical power method is probably least representative of corneal topography, while the tangential curvature method is more effective in assessing local areas of the cornea as in identifying the shape and the position of the cone in a keratoconic cornea but not in presenting an accurate global optical power estimate for the cornea. Lastly, both axial curvature and light ray tracing mapping methods are effective in representing the overall visual acuity as both consider the optical axis as a reference in the power calculations, however the latter method was not used since the numerical analysis errors associated with it are known to be condensed in the central optic zone, where topography data is most important (42).

Notable limitations of the study include its reliance on corneal topography and power, and the lack of consideration of the crystalline lens. This omission was necessary as the crystalline lens shape could not be determined accurately by existing Pentacam HR or another videokeratography technology. The crystalline lens characteristics may contribute to the overall eye astigmatism through the lenticular astigmatism component. However, it is expected that the contribution of this component will be small relative to that of the cornea due to the dominance of corneal power in determining visual acuity (25, 43). It is also important to acknowledge the studies suggested that repeatability of Scheimpflug devices can be lower for the posterior corneal surface than for the anterior corneal surface (44-46), however

measurements taken with the Pentacam are reported to be repeatable and reproducible when they obtained with the high-resolution settings and analysed with caution (47). This is beside the fact that, The Penntacam HR, unlike the Placido-based systems, can provide measurements for the posterior surface of the cornea which reported to have a significant effect on astigmatism magnitude and axis (45, 48).

Declaration of interest

All authors of this article declare that they have no conflict of interest.

Acknowledgements

We thank Dr Steve Jones, from the Ocular Biomechanics Group at the University of Liverpool, and Mrs Lynn White, the clinical director of UltraVision CLPL, for their comments that greatly improved the revised version of this manuscript.

This work was funded by an Innovate UK Knowledge Transfer Partnership programme grant 009521/UVP016.

References

1. Atchison DA, Charman WN. Thomas Young's contribution to visual optics: the Bakerian Lecture "on the mechanism of the eye". J Vis. 2010;10(12):16.

2. Henderson BA, Gills JP. A Complete Surgical Guide for Correcting Astigmatism: An Ophthalmic Manifesto: SLACK; 2011.

3. Rosenthal JW. Spectacles and Other Vision Aids: A History and Guide to Collecting: Norman Pub.; 1996.

4. Schellini SA, Durkin SR, Hoyama E, Hirai F, Cordeiro R, Casson RJ, et al. Prevalence of Refractive Errors in a Brazilian Population: The Botucatu Eye Study. Ophthalmic Epidemiology. 2009;16(2):90-7.

5. Liang YB, Wong TY, Sun LP, Tao QS, Wang JJ, Yang XH, et al. Refractive Errors in a Rural Chinese Adult Population: The Handan Eye Study. Ophthalmology. 2009;116(11):2119-27.

6. Saw SM, Goh PP, Cheng A, Shankar A, Tan DTH, Ellwein LB. Ethnicity-specific prevalences of refractive errors vary in Asian children in neighbouring Malaysia and Singapore. Br J Ophthalmol. 2006;90:1230-5.

7. Read S, Collins M, Carney L. A review of astigmatism and its possible genesis. Clin Exp Optom. 2007;90(1):5.

8. Tong L, Saw SM, Carkeet A, Chan WY, Wu HM, Tan D. Prevalence rates and epidemiological risk factors for astigmatism in Singapore school children. Optometry and Vision Science.79(9):606-13.

9. Jalie M. The principles of ophthalmic lenses. 5 ed. London, England: Association of Dispensing Opticians; 1972. 478 p.

10. Oshika T. Quantitative evaluation of corneal irregular astigmatism and wavefront aberrations. Cornea 2000;19(3):165-72.

11. Oshika T, Tomidokoro A, Maruo K, Tokunaga T, Miyata N. Quantitative evaluation of irregular astigmatism by Fourier series harmonic analysis of videokeratography data. Invest Ophthalmol Vis Sci. 1998;39(5):705-9.

12. Cavas-Martínez F, De la Cruz Sánchez E, Nieto Martínez J, Fernández Cañavate FJ, Fernández-Pacheco DG. Corneal topography in keratoconus: state of the art. Eye Vis. (London, England). 2016;3:5-.

13. Mannis MJ, Holland EJ. Cornea E-Book: Elsevier Health Sciences; 2016.

14. Hayashi K, Kawahara S, Manabe S-i, Hirata A. Changes in Irregular Corneal Astigmatism With Age in Eyes With and Without Cataract Surgery. Invest Ophthalmol Vis Sci. 2015;56(13):7988-98.

15. Oshika T, Tomidokoro A, Tsuji H. Regular and irregular refractive powers of the front and back surfaces of the cornea. Exp Eye Res. 1998;67:443-7.

16. Valencia-Estrada JC, Malacara-Doblado D. Parastigmatic corneal surfaces. Appl Opt. 2014;53(16):3438-47.

17. Tummanapalli SS, Potluri H, Vaddavalli PK, Sangwan VS. Efficacy of axial and tangential corneal topography maps in detecting subclinical keratoconus. J Cataract Refract Surg. 2015;41(10):2205-14.

18. Salmon TO, Horner DG. Comparison of elevation, curvature, and power descriptors for corneal topographic mapping. Optom Vis Sci. 1995;72(11):800-8.

19. Hickson-Curran S, Brennan NA, Igarashi Y, Young G. Comparative evaluation of Asian and white ocular topography. Optom Vis Sci. 2014;91(12):1396-405.

20. Hickson-Curran S, Young G, Brennan N, Hunt C. Chinese and Caucasian ocular topography and soft contact lens fit. Clin Exp Optom. 2016;99(2):149-56.

21. Lam CSY, Loran DFC. Designing contact lenses for oriental eyes Cont Lens Anterior Eye. 1991;14(3):109-14.

22. Cavas-Martinez F, De la Cruz Sanchez E, Nieto Martinez J, Fernandez Canavate FJ, Fernandez-Pacheco DG. Corneal topography in keratoconus: state of the art. Eye Vis (Lond). 2016;3:1-12.

23. Olsen T. On the calculation of power from curvature of the cornea. Br J Physiol Opt. 1986;70(2):152-4.

24. Ho J-D, Tsai C-Y, Tsai RJ-F, Kuo L-L, Tsai IL, Liou S-W. Validity of the keratometric index: Evaluation by the Pentacam rotating Scheimpflug camera. J Cataract Refract Surg. 2008;34:137-45.

25. Smit G, Atchison DA. The eye and visual optical instruments: Cambridge University Press; 1970.

26. Vojnikovi Bo, Tamajo E. Gullstrand's Optical Schematic System of the Eye Modified by Vojnikovi & Tamajo. Coll Antropol. 2013;37 (1):41-5.

27. Clark VL, Kruse JA. Clinical methods: the history, physical, and laboratory examinations. JAMA. 1990;264(21):2808-9.

28. Everitt BS, Skrondal A. The Cambridge Dictionary of Statistics: Cambridge University Press; 2010.

29. Villegas EA, Alcón E, Artal P. Minimum amount of astigmatism that should be corrected. J Cataract Refract Surg.40(1):13-9.

30. Yanoff M, Duker JS, Augsburger JJ. Ophthalmology: Mosby Elsevier; 2009.

31. Heidary G, Ying GS, Maguire MG, Young TL. The association of astigmatism and spherical refractive error in a high myopia cohort2005.

32. Maeda N, Klyce SD, Tano Y. Detection and Classification of Mild Irregular Astigmatism in Patients With Good Visual Acuity. Surv Ophthalmol. 1998;43(1):53-8.

33. Laíns I, Rosa AM, Guerra M, Tavares C, Lobo C, Silva MFL, et al. Irregular Astigmatism After Corneal Transplantation--Efficacy and Safety of Topography-Guided Treatment. Cornea. 2016;35(1):30-6.

34. Tanabe T, Tomidokoro A, Samejima T, Miyata K, Sato M, Kaji Y, et al. Corneal regular and irregular astigmatism assessed by Fourier analysis of videokeratography data in normal and pathologic eyes. Ophthalmology. 2004;111:752-7.

35. Borderie VM, Laroche L. Measurement of irregular astigmatism using semimeridian data from videokeratographs. J Refract Surg. 1996;12(5):595-600.

36. Valencia EJC, Malacara DD, Method for producing parastigmatic surfaces and lenses. EP patent WO2013089548 A3. 2013.

37. KLEIN SA. Axial Curvature and the Skew Ray Error in Corneal Topography. Optom Vis Sci. 1997;74(11):931-44.

38. Hua Y, Zhang X, Utheim TP, Huang J, Pan C, Tan W, et al. Evaluation of Equivalent Keratometry Readings Obtained by Pentacam HR (High Resolution). PLoS ONE. 2016;11(3):1-11.

39. Ambrósio R, Guerra FP, Araújo LPN, Khachikian SS, Belin MW, Iwanczuk J, et al. Elevation Based Corneal Tomography. 2 ed: Jaypee - Highlights Medical Publishers, Inc.; 2012.

40. Mannis MJ, Holland EJ. Cornea: Elsevier Health Sciences; 2016.

41. Oberkampf WL, Roy CJ. Verification and Validation in Scientific Computing: Cambridge University Press; 2010.

42. Khurana AK. Theory And Practice Of Optics And Refraction. 3 ed: Elsevier India Pvt. Limited; 2008.

43. Jogi R. Basic Ophthalmology. 4 ed. New Delhi: Jaypee Brothers,Medical Publishers Pvt. Limited; 2008.

44. Koch DD, Jenkins RB, Weikert MP, Yeu E, Wang L. Correcting astigmatism with toric intraocular lenses: effect of posterior corneal astigmatism. J Cataract Refract Surg. 2013;39(12):1803-9.

45. Preussner PR, Hoffmann P, Wahl J. Impact of Posterior Corneal Surface on Toric Intraocular Lens (IOL) Calculation. Curr Eye Res. 2015;40(8):809-14.

46. Schröder S, Eppig T, Langenbucher A. A Concept for the analysis of repeatability and precision of corneal shape measurements. Z Med Phys. 2016;26(2):150-8.

47. McAlinden C, Khadka J, Pesudovs K. A Comprehensive Evaluation of the Precision (Repeatability and Reproducibility) of the Oculus Pentacam HR. Invest Ophthalmol Vis Sci. 2011;52(10):7731-7.

48. Zhang B, Ma J-X, Liu D-Y, Guo C-R, Du Y-H, Guo X-J, et al. Effects of posterior corneal astigmatism on the accuracy of AcrySof toric intraocular lens astigmatism correction. Int J Ophthalmol. 2016;9(9):1276-82.

Table 1: Clinical data collected for normal and keratoconic eyes

Hospital	Hospital de Olhos Santa Luzia, Maceio, Alagoas, Brazil		Eye Hospital, WenZhou Medical University, Wenzhou, China	
Clinical diagnosis	Normal	Keratoconic	Normal	Keratoconic
Participants (eyes)	458	314	505	74
Age (mean ± SD) years	35.6 ± 15.8	31.6 ± 10.8	24.2 ± 5.7	22.0 ± 5.5
Age (min – max) years	10 – 87	10 – 72	17 – 48	11 – 41

Table 2: Clinical characteristics of normal and keratoconic eyes as measured by the Pentacam HR system

	Brazilian participants				Chinese participants			
Clinical diagnosis	Normal		Keratoconic		Normal		Keratoconic	
	$Mean \pm SD$	$Min: Max$	$Mean \pm SD$	$Min: Max$	$Mean \pm SD$	$Min: Max$	$Mean \pm SD$	$Min: Max$
Minimum corneal thickness (µm)	550±33	492:660	466±39	307:568	535±29	453:620	450±51	328:580
Flat curvature in the central 3 mm zone K1 (D)	42.6±1.4	39.4:46.6	44.7±3.1	36.7:55.3	42.8±1.4	38.2:48.1	47.0±5.0	36.7:62.6
Steep curvature in the central 3 mm zone K2 (D)	43.8±1.5	40.3:47.9	48.4±3.7	41.8:59.4	43.9±1.6	38.6:49.5	51.2±6.5	37.7:71.1
Mean curvature in the central 3 mm zone Km (D)	43.2±1.4	39.9:46.8	46.6±3.2	39.4:57.0	43.4±1.5	38.4:48.6	49.1±5.7	37.2:65.6
Index of surface variance in the central 8 mm zone ISV	20±5.8	8:46	71±31	17:155	16±4.7	7:59	87±42	14:186
Index of vertical asymmetry in the central 8 mm zone IVA	0.2±0.1	0.0:0.4	4.5±22.0	0.1:155.0	0.1±0.0	0.0:0.4	0.8±0.4	0.1:2.2
Keratoconus index in the central 8 mm zone KI	1.0±0.0	1.0:1.1	1.2±0.1	0.9:1.8	1.0±0.0	0.9:1.1	1.2±0.1	0.9:1.6
Central keratoconus index in the central 8 mm zone CKI	1.0±0.0	1.0:1.0	1.0±0.1	1.0:1.5	1.0±0.0	1.0:1.0	1.1±0.1	0.9:1.3
Index of height asymmetry in the central 8 mm zone IHA	4.1±3.2	0.1:15.5	23.7±17.5	0.3:70.9	3.7±2.9	0.0:18.6	31.8±27.5	0.2:160.4
Index of height decentration in the central 8 mm zone IHD	0.0±0.0	0.0:0.0	0.9±5.8	0.0:60.5	0.0±0.0	0.0:0.0	0.1±0.1	0.0:0.3
Irregularity index - based on Fourier analysis	0.03±0.01	0.01:0.07	0.04±0.01	0.01:0.08	0.02±0.01	0.01:0.14	0.04±0.02	0.01:0.18
Topographical keratoconus classification TKC (level)	NA	NA	2.1±0.7	1:3.5	NA	NA	2.6±0.8	1:3.5
Index of Bad D	0.4±0.5	-0.9:1.4	7.0±3.3	1.5:20.8	1.0±0.6	-0.8:3.0	9.4±5.4	0.4:24.6

Table 3: Acute angle and absolute power difference between steepest and flattest meridians determined for Brazilian and Chinese eyes using orthogonal and non-orthogonal analysis

Analysis methods	Brazilian participants				Chinese participants			
	Acute angle φ $Mean \pm SD$ (Degree)		Abs power difference ΔP $Mean \pm SD$ (Dioptre)		Acute angle φ $Mean \pm SD$ (Degree)		Abs power difference ΔP $Mean \pm SD$ (Dioptre)	
	Normal	Keratoconic	Normal	Keratoconic	Normal	Keratoconic	Normal	Keratoconic
Orthogonal	90.0±0.0		1.1±0.8	3.3±2.3	90.0±0.0		0.8±0.5	4.8±2.6
Non-orthogonal (range)	73.7±13.1 (31 : 90)	82.5±8.2 (45 : 90)	1.2±0.7 (0.1 : 4.7)	3.4±2.2 (0.3 : 11.8)	70.6±13.5 (32 : 90)	85.4±4.8 (67 : 90)	0.9±0.5 (0.1 : 3.4)	4.8±2.6 (0.7 : 10.7)
Difference	-16.4±13.1	-7.5±8.2	0.07±0.10	0.03±0.00	-19.4±13.5	-4.6±4.8	0.08±0.08	0.02±0.05
Significance (p)	0.000	0.000	0.190	0.870	0.000	0.000	0.015	0.960

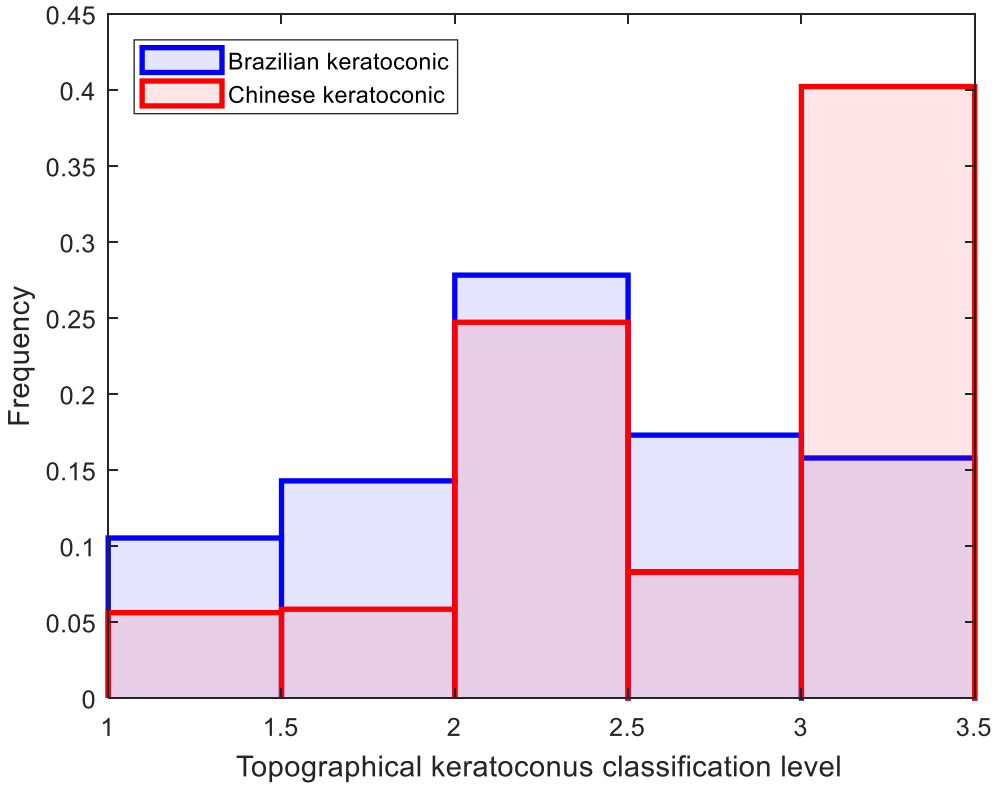

Figure 1: Topographical keratoconus classification level for keratoconic patients as identified by the Pentacam HR (unclassified keratoconic cases were 0.14 of Brazilian participants and 0.15 of Chinese participants).

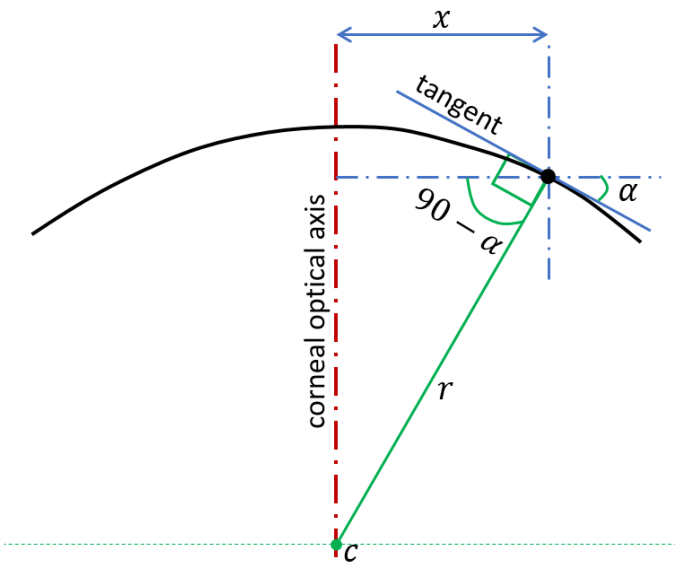

Figure 2: Determination of corneal surface axial radius of curvature (r) in a certain meridional plane. In this method, the centre of curvature (c) is always restricted to lay on the cornea's optical axis.

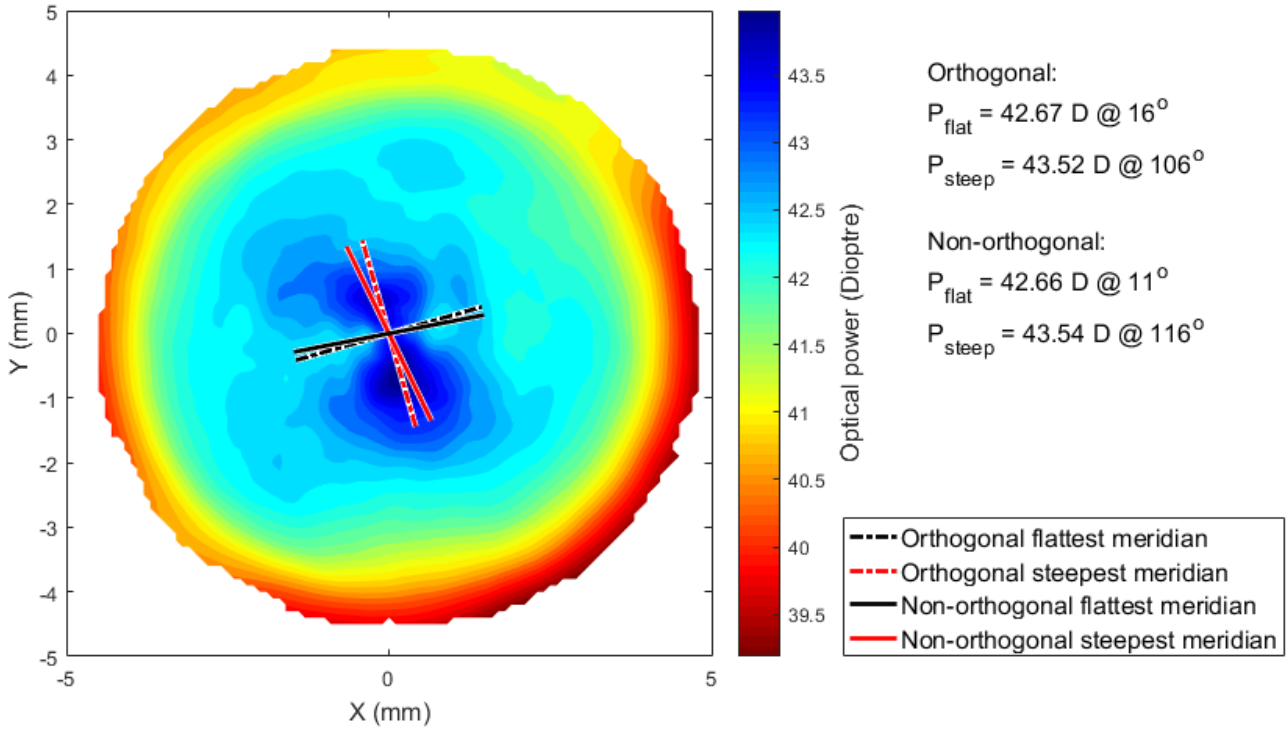

Figure 3: Optical power map for a left eye of a normal Chinese participant (female 26 years old) based on the axial curvature method. The map shows the orthogonal and non-orthogonal power meridians.

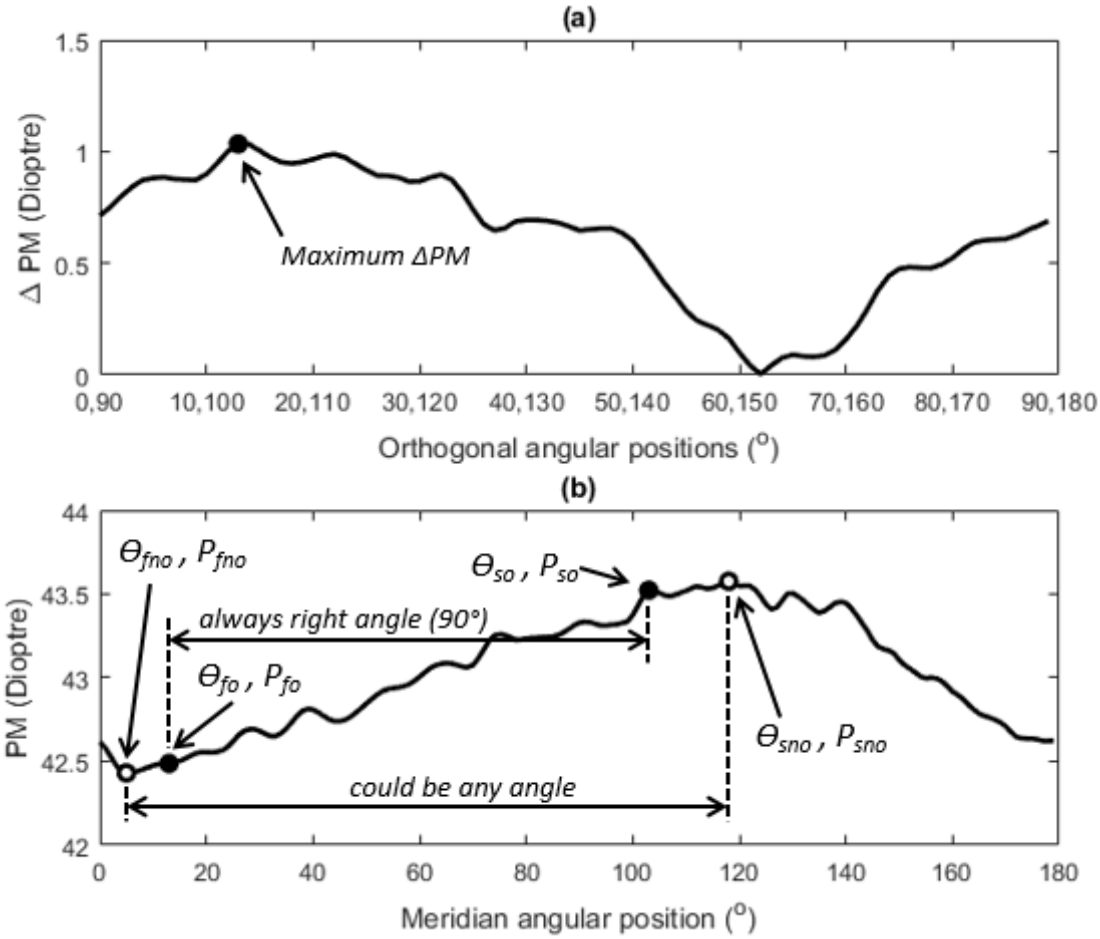

Figure 4: Calculating the position of flattest and steepest power meridians – P_{fo}: power of flattest orthogonal meridian; Θ_{fo}: angular position of flattest orthogonal meridian, P_{so}: power of steepest orthogonal meridian, Θ_{so}: angular position of steepest orthogonal meridian, P_{fno}: power of flattest non-orthogonal meridian, Θ_{fno}: angular position of flattest non-orthogonal meridian, P_{sno}: power of steepest non-orthogonal meridian, Θ_{sno}: angular position of steepest non-orthogonal meridian.

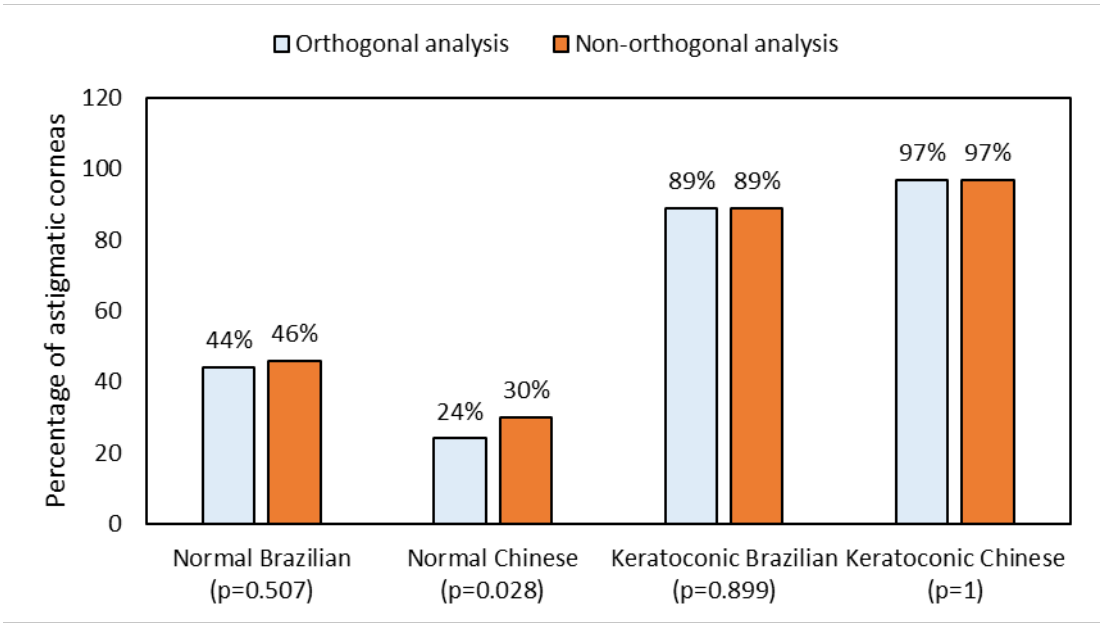

Figure 5: Astigmatism based on orthogonal and non-orthogonal power axes analysis among the four populations.

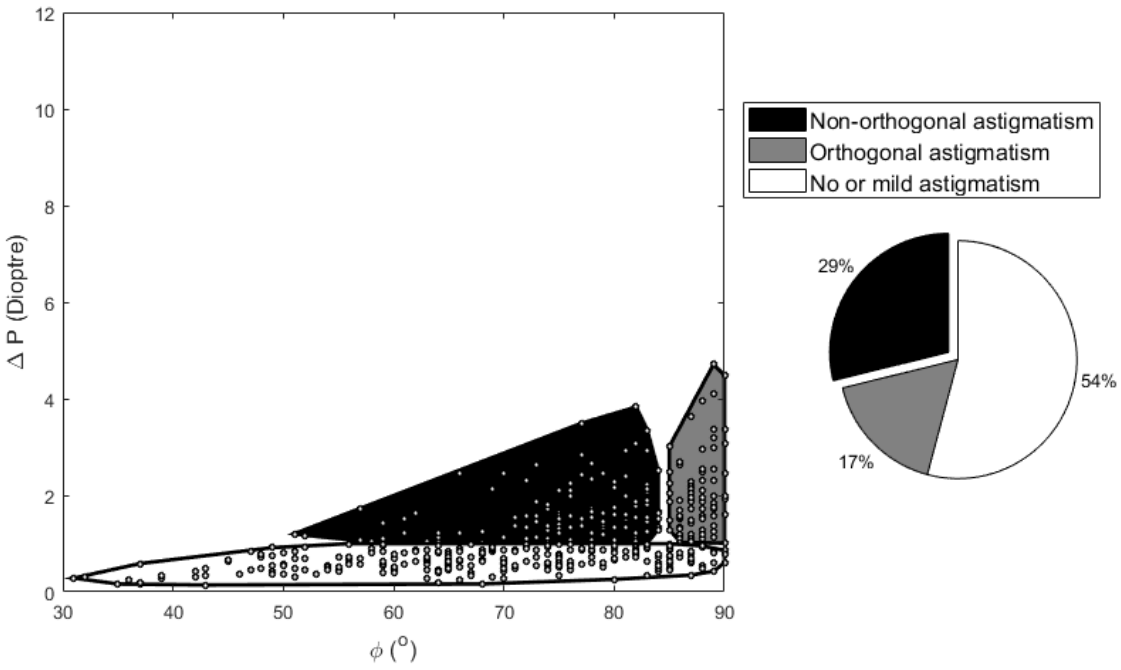

(A)

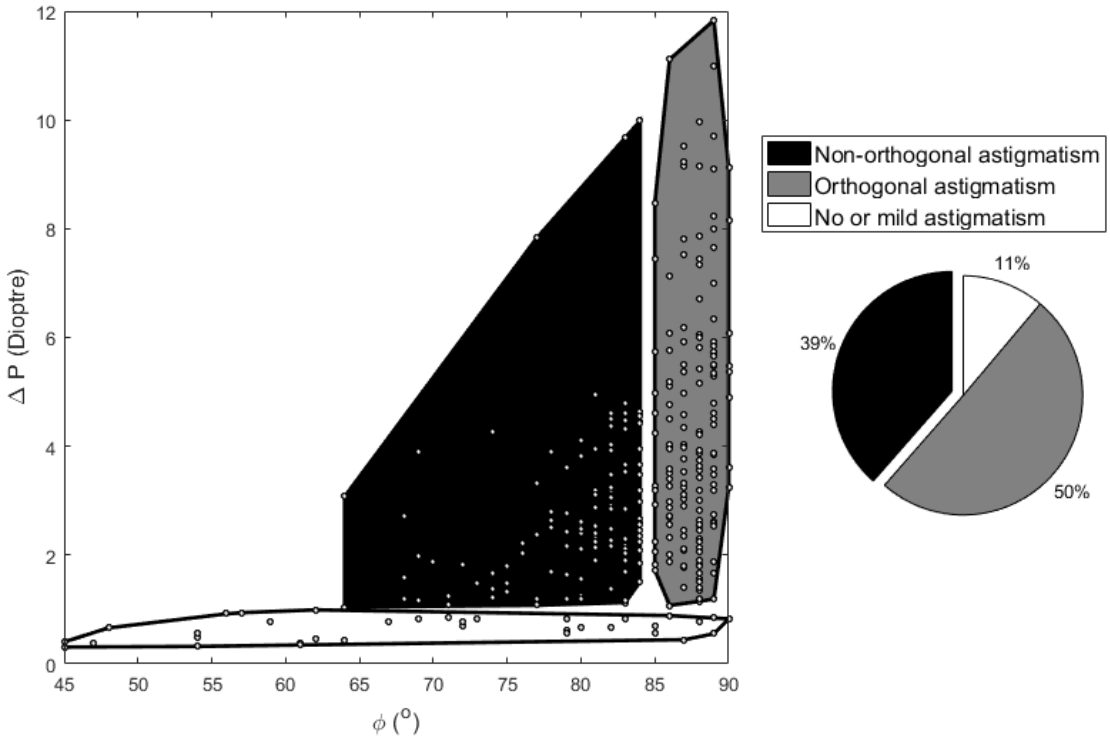

(B)

Figure 6: Acute angular difference between the cornea's flattest and steepest power meridians plotted against the power difference for Brazilian normal (A) and keratoconic (B) participants.

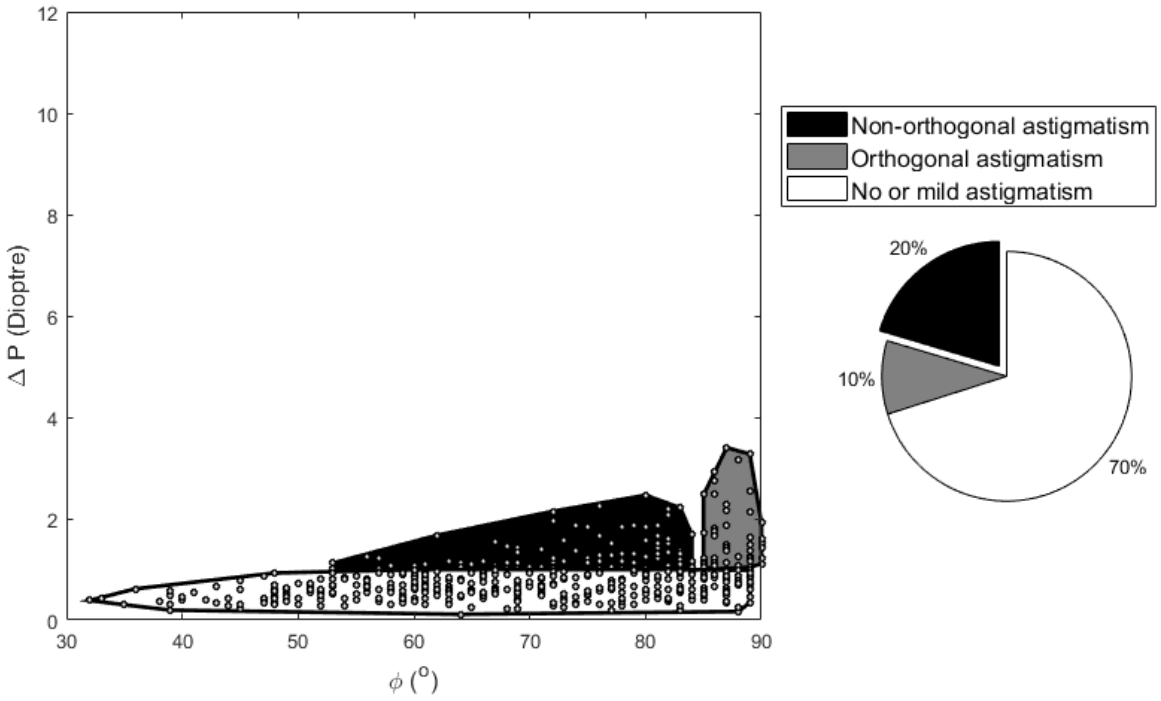

(A)

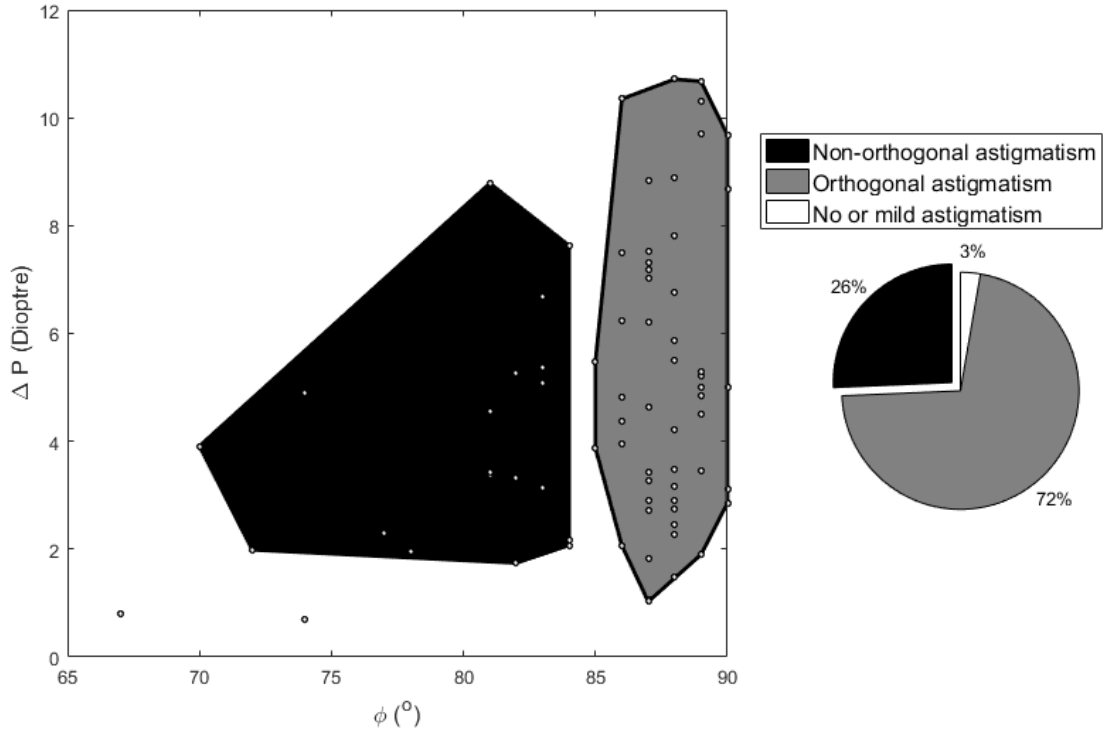

(B)

Figure 7: Acute angular difference between the cornea's flattest and steepest power meridians plotted against the power difference for Chinese normal (A) and keratoconic (B) participants.